Journal of Molecular Catalysis B: Enzymatic 61 (2009) 225–234

Contents lists available at ScienceDirect

Journal of Molecular Catalysis B: Enzymatic

journal homepage: www.elsevier.com/locate/molcatb

Differences in biocatalytic behavior between two variants of StcI esterase from *Aspergillus nidulans* and its potential use in biocatalysis

Carolina Peña-Montes[a,b], Stefan Lange[b], Denise Castro-Ochoa[a], Katia Ruiz-Noria[a], Felipe Cruz-García[c], Rolf Schmid[b], Arturo Navarro-Ocaña[a], Amelia Farrés[a,*]

[a] *Food and Biotechnology Department, Chemistry Faculty, National Autonomous University of Mexico (UNAM), Ciudad Universitaria, Mexico City, D.F. 04510, Mexico*
[b] *Institute of Technical Biochemistry, University of Stuttgart, Stuttgart, Germany*
[c] *Biochemistry Department, Chemistry Faculty, National Autonomous University of Mexico (UNAM), Ciudad Universitaria, Ciudad Universitaria, Mexico City, D.F. 04510, Mexico*

ARTICLE INFO

Article history:
Received 17 April 2009
Received in revised form 13 July 2009
Accepted 22 July 2009
Available online 30 July 2009

Keywords:
Aspergillus nidulans
Esterase
Biocatalysis
Sterigmatocystin
N-terminus
Phenolic compounds

ABSTRACT

Aspergillus nidulans produces the esterase StcI, which is involved in the biosynthesis of sterigmatocystin, a precursor of aflatoxins. Analysis of ESTs indicated the presence of an additional 29-amino acid N-terminal region of the already reported *stcI* gene. Predicted structural models suggest that this N-terminus modifies substrate access to the active site. In order to elucidate the role of this N-terminal region, the complete gene (*nstcI*) and the truncated reported version of the gene (*stcI*) were cloned and expressed in *Pichia pastoris*. Both recombinant enzymes were tested for their ability to hydrolyze *p*-nitrophenyl esters and compounds having a structure similar to the original substrate. We observed differences in the abilities of these two enzymes to hydrolyze *p*-NPE. The ratios between the activity of the two esterase versions (NstcI/StcI) towards different acyl chain-length *p*-NPE were: 9.3 towards *p*-NPA (C2:0); 0.76 towards *p*-NPB (C4:0) and *p*-NPD (C10:0); 1 towards *p*-NPL (C12:0) and *p*-NPM (C14:0); 2.7 towards *p*-NPP (C16:0) and 2.2 towards *p*-NPS (C18:0). Interestingly, NstcI esterase showed the highest activity (366 U/mg protein) towards *p*-NPA (C2:0) and StcI towards *p*-NPS (C18:0) (77 U/mg protein). Different deacetylation reactions of bioactive compounds were also assayed. The results indicated differences in chemoselectivity for deacetylation of phenols, kojic acid and flavonoid esters. Acetylated ferulic acid was efficiently hydrolyzed (96%) only by NstcI, while deacetylation of coumaric acid was done only by StcI (25%). Deacetylation of kojic acid was carried out only by NstcI (75%). Almost all flavonoids were efficiently deacetylated by NstcI with 100% of conversion with the exception that epicatechin was hydrolyzed 60%. In contrast, low conversion of acetylated flavonoids was obtained with StcI (15–20%), the highest value was observed with catechin, 63%. We also observed differences in regioselectivity for the deacetylation of kojic acid and flavonoids. This behavior suggests an important role for the N-terminus in the catalytic properties of this enzyme. In addition, these enzymes showed different versatile catalytic potential in terms of chemo- and regioselectivity in carrying out a variety of industrially important biotransformations of phenolic compounds.

1. Introduction

An esterase/lipase putative gene (*stcI*) has been reported in the sterigmatocystin pathway gene cluster in *Aspergillus nidulans* [1]. This gene is homolog to the *estA* gene, which was identified within the aflatoxin pathway gene cluster in *Aspergillus parasiticus*. The esterases encoded by the *estA* and *stcI* genes share 49% amino acid identity which is within the range of homology between aflatoxin and sterigmatocystin biosynthetic pathway genes in *A. parasiticus* and *A. nidulans* [2]. The esterase EstA converts versiconal hemiacetal acetate (VHA) to versiconal (VAL) and versiconol acetate (VOAc) to versiconol (VOH) [3]. The nature of the reaction catalyzed by this enzyme, i.e. deacetylation, suggests that StcI may have the biocatalytic potential to perform reactions with high enantio- or regioselectivity for cyclic substrates.

Abbreviations: ST, sterigmatocystin; VHA, versiconal hemiacetal acetate; VHOH, versiconal; VOAc, versiconol acetate; VAL, versiconal; VOH, versiconol; EST, expression sequence tag; PCR, polymerase chain reaction; DTT, dithiothreitol; α-NA, α-naphthyl acetate; *p*-NPE, *p*-nitrophenyl esters; *p*-NPA, *p*-nitrophenyl acetate; *p*-NPB, *p*-nitrophenyl butyrate; *p*-NPD, *p*-nitrophenyl decanoate; *p*-NPL, *p*-nitrophenyl laurate; *p*-NPM, *p*-nitrophenyl myristate; *p*-NPP, *p*-nitrophenyl palmitate; *p*-NPS, *p*-nitrophenyl stearate; RT, room temperature; OD, optical density; SDS, sodium dodecyl sulphate.

* Corresponding author at: Departamento de Alimentos y Biotecnología, Facultad de Química, Universidad Nacional Autónoma de México, Ciudad Universitaria, Mexico City, D.F. 04510, Mexico. Tel.: +52 55 56225305; fax: +52 55 56225309.
E-mail address: farres@servidor.unam.mx (A. Farrés).

1381-1177/$ – see front matter © 2009 Elsevier B.V. All rights reserved.
doi:10.1016/j.molcatb.2009.07.009

In the cDNA *A. nidulans* Sequencing Project [4], there are two EST sequences for StcI protein: CONTIG1592, which corresponds to the previously reported C-terminal region [1], and CONTIG452, which corresponds to the N-terminal region. We found an additional 29-amino acid region at the N-terminus of the protein, which is not homologous to any signal peptide [5]. Predicted structural models for the already reported protein (StcI) and StcI with the additional 29-amino acid region (NstcI) suggest that this N-terminus can modify the substrate access to the active site. In order to elucidate the role of this N-terminal domain, we have cloned and characterized both esterase forms in *Pichia pastoris*.

Phenolic derivatives are found in both edible and non-edible plants, may act as antioxidants, chelating agents, and free radical scavengers, and may have anti-inflammatory, antiallergenic, antimicrobial, antiviral, anticarcinogenic, and UV filtration properties [6,7]. Along with flavonoids, they have been considered important agents in the prevention of cancer and heart disease [8,9]. Applications for these natural antioxidants in oil-based food processing and cosmetics are limited because of the relatively low solubility of phenolic acids in aprotic media. To increase biological activity, it is necessary to chemically modify the naturally found compounds by acetylation, deacetylation or glycosylation. As such, the hydrophobicity of phenolic acids can be enhanced by chemical or enzymatic lipophilization by esterifying the carboxylic acid function of the phenolic acid with a fatty alcohol to obtain an amphiphilic molecule, which should keep its original functional properties [10]. Chemical modification is not highly selective, while among industrially important enzymes lipases and esterases are particularly valuable because of their chemo-, regio- and enantioselective capabilities [11–13] with the added advantage that unwanted functionalization of phenolic hydroxyl groups is avoided [14]. This enzyme reaction has been reported specifically for some flavonoids, but only a few biocatalysts can deacetylate phenolic compounds, to render them more bioactive [15–19]. As such, the most widely used enzyme is produced by *Candida antarctica* (Novozym 434). Therefore, it is important to evaluate new enzymes to perform lipophilization, regioselective reactions and potential reverse reactions to obtain more interesting compounds or to increase yields. In this work, the behavior of both recombinant forms of StcI esterase during the deacetylation of interesting industrial compounds is also analyzed.

2. Materials and methods

2.1. Microorganisms, plasmid, media and culture conditions

The *stcI* and *nstcI* genes were isolated from a 24 h developmental *A. nidulans* cDNA library in λ-ZAPII constructed by R. Aramayo, available from the Fungal Genetics Stock Center, Kansas City, KS.

E. coli DH5α (F^- ϕ80d*lac*ZDM15Δ (*lac*ZYA-argF) U169 *end*A1 *rec*A1 *hsd*R17($r_K- m_K+$) *deo*R *thi*-1 *sup*E44 λ-*gyr*A96 *rel*A1) was used for cloning. *P. pastoris* X-33 (wild type) (Invitrogen, Carlsbad, CA) was used for enzymatic expression. Plasmid pPICZαB was supplied from Invitrogen (Carlsbad, CA).

P. pastoris growth, media and selection of recombinant clones were performed according to the techniques described in the manual of EasySelect *Pichia* expression kit (Version G) (Invitrogen, Carlsbad, CA). Enzyme-producing clones were selected on YEPD medium supplemented with 0.5% (w/v) dextrose, 1% (v/v) tributyrin and 100 μg/mL zeocin (YEPT medium).

2.2. Construction of the plasmids pPICZαstcI and pPICZαnstcI

The vector pPICZαB was used to achieve extracellular expression in *P. pastoris*. Two restriction sites (PstI/NotI) were introduced into the fragment by PCR. The *nstcI* gene was amplified from cDNA with the primers *nstcI*-F and *stcI*-R to generate the desired gene region which contains the additional 29 amino acids in the N-terminal end. The Hotstart Taq DNA polymerase (Qiagen, Valencia, CA) was used in these PCR experiments. The sequences of the primers were: Forward-1, *nstcI*-F, 5′-CCT CTG CAG CAG ATT CCA AGC TAT CAG AGC CAT G-3′ and reverse, *stcI*-R, 5′-TGA GCG GCC GCT TAC TCA CAA ACC CAG C-3′. The PCR amplification was carried out as follows: an initial denaturation step at 95 °C for 2 min, followed by 95 °C for 1 min, 55 °C for 40 s and 72 °C for 1.5 min for 30 cycles; and a final extension step at 72 °C for 10 min. The PCR fragments were cleaved with restrictions endonucleases PstI and NotI and inserted into the respective sites of pPICZαB, resulting in pPIC*nstcI* vector.

In order to clone the truncated version of the *stcI* gene (without the additional 29 amino acids in the N-terminal region) into *P. pastoris*, the same restriction sites were used. For PCR amplification, the forward primer *stcI*-F was used instead of *nstcI*-F. Primers had the following sequences: Forward-2, *stcI*-F, 5′-CCT CTG CAG CAC AGG GAT GGA AGA CGA TAG-3′ and reverse, *stcI*-R, 5′-TGA GCG GCC GCT TAC TCA CAA ACC CAG C-3′. Recombinant Pfu polymerase (Fermentas, Hanover, USA) was used in these PCR experiments. A gradient PCR was performed with the following cycle conditions: an initial denaturation step at 95 °C for 2 min, followed by 95 °C for 1 min, 50–60 °C gradient for 40 s and 72 °C for 1 min 30 s for 25 cycles; and a final extension step at 72 °C for 10 min.

2.3. Recombinant DNA techniques

Standard recombinant DNA methods were carried out as described by Sambrook et al. [20].

2.4. Cloning into E. coli

DH5α competent cells were freshly transformed with the vectors pPICZα*stcI* and pPICZα*nstcI* by electroporation. Selected recombinant clones were grown at 37 °C in 50 mL LB media for vector extraction with a plasmid midi kit (Qiagen, Valencia, CA).

2.5. Expression of StcI and NstcI in P. pastoris

P. pastoris X-33 cells were freshly transformed with the expression vectors pPICZα*stcI* and pPICZα*nstcI* by means of electroporation. Negative control cells were also transformed with pPICZαB. All cultures were incubated at 30 °C. Recombinant clones were selected on YEPD medium, and halo-producing clones were selected on YEPT medium. For negative control cells, we have obtained nonhalo-producing clones. Negative control cells and positive transformants were cultured in 25 mL of buffered glycerol-complex medium (BMGY) shaken at 28 °C and 250 rpm in 250 mL glass flasks. When cultures reached an OD_{600} = 2–6, the cells were centrifuged (3000 × *g*, 15 min) and resuspended in 50 mL buffered methanol-complex medium (BMMY) to an OD_{600} of 1, shaken at 28 °C and 250 rpm in 250 mL glass flasks for 96 h. Induction of esterase expression was achieved by daily addition of 100% methanol to a final concentration of 0.5%. After induction, *Pichia* cells were removed by centrifugation (3000 × *g*, 15 min), and supernatant was collected. Desalting, concentration (42-fold) and buffer exchange to PBS, pH 7.4 of supernatant was done by ultrafiltration (Amicon, Beverly, MA) through a 10-kDa membrane (Millipore, USA). The concentrated solution was used for SDS-PAGE and esterase activity assay.

2.6. Purification of recombinant proteins by immunoaffinity column

StcI PAb were generated in rabbits by Sigma-Genosys and targeted to the StcI sequence, using a synthetically designed peptide

Fig. 1. StcI genomic and deduced amino acid sequences. *stcI* DNA and coding sequence. The deduced amino acid sequence is presented under the corresponding codons. They are numbered on the right side. In the promoter region, the *aflR* binding consensus (the canonical $TCGn_5CGA$ binding site), CAAT sequences are underlined. Intron sequence is denoted by cursive lowercase letters. PCR primers are bold and labeled. The amino acids from the catalytic triad (Ser-152, Asp-255 and His-285) and oxyanion hole (Gly-86 and Ala-153) are bold and underlined. Designed peptide sequence is enclosed.

as the antigen by Sigma-Genosys (The Woodlands, TX) (Fig. 1). Specificity was assayed by western blotting as described in manual of polyscreen PVDF transfer membrane improved (Perkin–Elmer Life Sciences, Boston, MA), using semi-dry method. StcI antiserum after 77 days of immunization was tested at dilution of 1:40,000. Preimmune serum had no reactivity. Antibodies were purified using the Montage Antibody Purification Prosep-A kit, according to the techniques described in the manual (Millipore Corp., Bedford, MA). Purified antibodies (20 mg) were immobilized to Affi-Gel-10 (Bio-Rad, Hercules, CA), as recommended by the manufacturer. Purification of recombinant proteins was done according to the manual for activated immunoaffinity supports (Bio-Rad, Hercules, CA) using an acid elution with sodium citrate, 0.15 M, pH 3. Briefly, 1 mL of concentrated supernatant was applied to immunoaffinity column pre-equilibrated with PBS buffer. Non-bounded proteins were eluted with 3 bed volumes of Triton X-100 (0.5%) in PBS. Recombinant protein was eluted with 2 bed volumes of sodium citrate buffer. Collected fractions were neutralized to pH 7. Desalting, concentration and buffer exchange to sodium phosphate, 0.1 M, pH 7.5 of the collected fractions was done by ultrafiltration using a membrane with a molecular mass exclusion limit of 10 kDa (Millipore Corp., Berford, MA). Sample was assayed for esterase activity. Affinity column was regenerated by 5 bed volumes of PBS and 2 of sodium azide (0.02%) in PBS.

2.7. Fast hydrolase activity assay

Esterase activity of the crude extracts and purified enzymes was measured spectrophotometrically towards *p*-NPA in accordance with Isobe et al. with some modifications [21]. Esterase, 100 μL, was added to 900 μL of reaction buffer containing 50 mM potassium phosphate, pH 7.2, 1% Triton X-100 and 2.5 μM of *p*-NPA. The reaction was carried out at 25 °C and 1 U of enzyme activity was defined as the quantity of enzyme that releases 1 μmol of *p*-nitrophenol per minute at 37 °C. Absorbance was continuously measured at 410 nm.

2.8. Protein determination

Protein concentration was determined by Bradford assay (Bio-Rad, Hercules, CA) using the enhanced method according to the manufacturer's instructions and bovine serum albumin as the standard.

2.9. Polyacrylamide gel electrophoresis

SDS-PAGE on a 12% polyacrylamide slab gel was used to assess the purity and molecular weight of the enzyme according to the method proposed by Laemmli [22]. Low molecular weight markers (BioRad) were used as standards.

2.10. Zymogram

Esterase activity was assayed and visualized using zymograms. After SDS-PAGE, the acrylamide gel was washed by immersion in phosphate buffer 0.1 M, pH 7.5 for 30 min with constant agitation. For renaturation of the enzyme, a second wash was performed in the same conditions, with the exception that the buffer contained 5% Triton X-100. Finally, the gel was subjected to a third wash in the same buffer with only 0.5% Triton X-100 for 4 h. For detection of esterase activity, the gels were incubated at RT in substrate solution for 10 min (3 mM α-naphthyl acetate, 10% (v/v) acetone and 100 mM sodium phosphate buffer, pH 7.5) and then incubated for 5 min in developing solution (1 mM Fast Red TR, 0.1% (v/v) Triton X-100 and 100 mM sodium phosphate buffer, pH 7.5). Esterase activity was visualized by the appearance of purple-colored bands in the gels.

2.11. Bioinformatics

stcI gene sequence data were manually compiled from GenBank. BLAST searches were performed within the *A. nidulans* initiative genome database of the Whitehead Institute [23]. *StcI* ESTs

were identified using BLAST searches within the *A. nidulans* cDNA Sequencing Project [4]. The sequences were analyzed using the following programs: DNA strider [24], ClustalW [25], BioEdit Version 7.0.7 [26], Genefinder [27], Genescan [28] and Expasy Translate Tool [29]. The prediction of signal peptides was done using Signal P v3 [5]. Prediction of the structure model was performed using the EsyPred3D Program [30]. The predicted structure was verified with the program WHAT IF [31].

The selection for the template was performed using the fold recognition and identification of distant homologues method, mGenTHREADER [32]. This program makes use of profile–profile alignments and predicted secondary structure (using PSIPRED) as inputs [33]. This increases both the sensitivity of the method and enhances the accuracy of alignments. According to this program the closest homologues of NstcI are the heroin esterase from *Rhodococcus* sp. (19% amino acid sequence similarity) [34] and a thermophilic esterase from *Alicyclobacillus acidocaldarius* (30% amino acid sequence similarity) [35]. Therefore, the crystallographic structure of the heroin esterase and carboxylesterase (PDB code 1LZL and 1QZ3) were used as templates for homology modeling of NstcI and StcI enzymes.

2.12. Biochemical characterization

Temperature and pH optima for the assayed conditions were determined by a spectrophotometric method as previously described by Isobe et al. [21] and by a pH-stat assay according to Peled and Krenz [36], using 200 mM ethyl butyrate, which ensured a large excess of substrate, in a pH-stat apparatus (Titrino®, Metrohm, Switzerland). To study the effect of temperature, enzymatic activity was assayed at 20, 30, 40, 50 and 60 °C at pH 7.5 (0.1 M phosphate buffer) for 15 min with applicable controls. Thermostability of the esterase was investigated by quantifying the remaining activity after incubating the enzyme without substrate in 0.1 M phosphate buffer, pH 7.5, at various temperatures (20–60 °C) during 30 min and then assaying its activity at 25 °C. Triplicates were performed for each reaction, and the values were corrected for the non-catalyzed hydrolysis of the substrate.

The pH optimum was assayed during 30 min at 37 °C in a pH range from 5 to 10 in the following buffers: 50 mM acetate (pH 5), 50 mM sodium phosphate buffer (pH 6–7) and 50 mM Tris–HCl (pH 8–10). The effect of the pH on enzyme stability was determined by incubating esterase solution in buffers (50 mM, pH 5–10) for 12 h at 37 °C. After incubation, the pH values remained constant, and residual activity was evaluated by spectrometric and pH-stat methods. Triplicates were performed for each reaction, and the values were corrected for the non-catalyzed hydrolysis of the substrate.

2.13. Chain-length specificity of recombinant esterases

Fatty acid *p*-nitrophenyl derivatives and ethyl esters were used as substrates. (i) *Spectrophotometric analysis*: For *p*-nitrophenyl-fatty acyl esters, acyl group chain-lengths from C2:0 to C18:0 were tested as previously described [21]. (ii) *pH-stat assay*: It was performed using different ethyl esters with acyl group chain-lengths from C4:0 to C16:0 and aromatic groups at optimum assay conditions as described previously [36]. Triplicates were performed for each reaction and were corrected for the non-catalyzed hydrolysis of the substrate.

2.14. Preparation of acetylated compounds

The acetylated compounds were prepared under standard conditions using acetic anhydride and pyridine. Specifically, a mixture of phenolic compound (100 mg), acetic acid anhydride (3 mL) and pyridine (3 mL) was warmed at 60 °C for 45 min. The reaction mixture was evaporated to dryness under N_2, was poured into ice-cold dilute hydrochloride acid (5 mL) and was extracted with ethyl acetate (2× 5 mL). A fraction was used for the hydrolysis reactions.

2.15. Enzyme conditioning

The crude extracts from recombinant *P. pastoris* (transformed with pPICZα*stcI*, pPICZα*nstcI* and pPICZαB) were centrifuged at 3000 × *g* for 15 min and the supernatant was collected and lyophilized. An enzyme solution containing 2 mg/mL of protein was prepared by the dissolution of the lyophilized extract in phosphate buffer pH 7 at a concentration of 50 mM and was tested for its esterase activity by spectrophotometry using *p*-NPA as substrate.

2.16. Enzymatic deacetylation

Acetylated compounds were divided into three groups according to their structure: phenols (I), aliphatic alcohols (II) and flavonoids (III). For this, 15 mg of the acetylated compound were dissolved in 1.1 mL of solvent (acetone or toluene), and 400 μL of enzyme was then added. The volume was adjusted to 3.5 mL with 0.05 M sodium phosphate buffer, pH 7. The reaction mixture was stirred for 48 h at 37 °C and 200 rpm. The degree of conversion was monitored by thin layer chromatography and HPLC. A reaction without enzyme was evaluated for autohydrolysis of all tested acetylated compounds. Upon completion, 2 mL of ethyl acetate was added for product extraction. The organic phase was separated, and the solvent was evaporated to dryness at 37 °C.

2.17. Identification of compounds

All reaction products were fully characterized on the basis of their physical and spectral data. Melting points were determined using a MEL-TEM and were uncorrected. Thin layer chromatography (TLC) was used for analysis of product formation. A solvent system was chosen according to the substrate. The plates were developed using a saturated iodine chamber or by spraying with 10% H_2SO_4, when aliphatic alcohols were tested. A free radical scavenging assay to test antioxidant activity of phenols was performed using the stable free radical DPPH (1, 1-diphenyl-2-picryhydrazyl) [37]. Gas chromatography (GC) was performed in an Agilent Technologies 6890N Network GC system, Injector 7683, using a 30 m DB-5MS column with 0.25 mm inner diameter and 0.25 μm film thickness. The temperature range was 60–325 °C. Acetylated and non-acetylated standards were also assayed. HPLC was performed in a Waters 1525 HPLC system, and the reaction mixture was separated on a 3.9 mm × 155 mm Waters Symmetry® C185 μm column. An elution system consisting of methanol and acetic acid (1%) was used. The products were purified by silica column chromatography (mesh size 100–200 μm) and analyzed on the basis of nuclear magnetic resonance (NMR). The nuclear magnetic resonance (NMR) spectra were measured in $CDCl_3$ a 300 K on a VarianVXR-300S spectrometer operating at 300 MHz (^{1}H) and 100 MHz (^{13}C). Approximately 25 mg of **1a**–**1j** (Fig. 8) were dissolved in $CDCl_3$, with tetramethylsilane (TMS) as internal standard. The structures were identified by direct comparison of spectral properties. MS and ^{1}H NMR are in agreement with those of the authentic compounds in the literature. The ^{13}C NMR data obtained for acetylated compounds (**1a**–**1j**) (Fig. 8) were compatible with the literature data. We include the ^{13}C NMR data for all acetylated compounds (**1a**–**1j**) but they were characterized also on the basis of ^{1}H NMR, EM and melting point.

^{13}C NMR for 4-O-acetyl-ferulic acid (**1a**): δ = 169.12, 167.75, 148.15, 146.43, 145.42, 126.31, 123.22, 115.14, 109.45, 56.07, 20.65.

^{13}C NMR for 2-O-acetyl-α-naphtol (**1b**): δ = 169.51, 146.72, 134.72, 128.12, 126.51, 126.51, 126.09, 121.21, 118.16.

^{13}C NMR for 1,4-O-diacetyl-2-*ter*-butyl-hidroquinone (**1c**): δ = 169.42, 169.35, 147.81, 142.46, 124.69, 120.35, 119.74, 34.58, 29.97, 21.59, 21.11.

^{13}C NMR for 4-O-acetyl-coumaric acid (**1d**): δ = 171.30, 169.10, 152.88, 131.75, 129.51, 122.23, 117.27, 21.13.

^{13}C NMR for 1,4-O-diacetyl-hydroquinone (**1e**): δ = 169.47, 147.72, 120.75, 21.16.

^{13}C NMR for 1-O-acetyl-2-phenylethanol (**1f**): δ = 170.96, 137.83, 128.89, 128.50, 126.56, 64.92, 35.10, 20.94.

^{13}C NMR for 5, 1′-O-diacetyl-kojic acid (**1g**): δ = 172.06, 169.53, 167.49, 162.18, 147.69, 141.01, 114.19, 60.72, 20.31, 20.14.

^{13}C NMR for 3-0-acetyl-β-amyrin (**1h**): δ = 170.98, 145.19, 121.63, 80.93, 55.25, 47.55, 47.23, 46.78, 41.71, 39.81, 38.26, 37.71, 37.14, 36.84, 34.73, 33.33, 32.59, 32.49, 31.08, 28.39, 28.03, 26.93, 26.14, 23.57, 23.53, 21.30, 18.26, 16.80, 16.69, 15.55.

^{13}C NMR for 3-O-acetyl-dihydrocholesterol (**1i**): δ = 170.69, 73.78, 56.42, 56.27, 54.24, 44.66, 42.58, 39.99, 39.52, 36.76, 36.17, 35.48, 35.46, 34.04, 31.96, 28.24, 28.01, 27.48, 24.21, 23.84, 22.81, 22.56, 21.47, 21.20, 18.67.

^{13}C NMR for quercetin pentaacetate (**1j**): δ = 170.54, 169.76, 168.35, 168.31, 168.29, 168.23, 157.32, 154.75, 154.28, 150.86, 144.86, 142.68, 134.52, 128.19, 126.89, 124.40, 124.31, 115.23, 109.46, 21.64, 21.50, 21.13, 20.98.

^{13}C NMR for hesperetin tetraacetate (**1k**): δ = 189.05, 169.24, 168.84, 167.94, 163.14, 155.89, 151.58, 151.18, 139.89, 130.54, 124.84, 121.02, 112.47, 111.72, 110.51, 109.08, 78.77, 56.01, 44.87, 21.13, 21.02, 20.68.

^{13}C NMR for (+)catechin pentaacetate (**1l**): δ = 170.23, 169.05, 168.46, 168.16, 154.50, 149.99, 149.55, 142.24, 142.22, 136.26, 124.52, 123.83, 121.90, 110.31, 108.90, 107.80, 77.78, 68.40, 24.96, 21.22, 21.08, 20.91, 20.77, 20.75.

^{13}C NMR for (−)epicatechin pentaacetate (**1m**): δ = 170.42, 168.98, 168.42, 168.09, 168.04, 154.96, 149.73, 149.67, 142.00, 141.88, 135.84, 124.36, 123.29, 122.03, 109.68, 108.74, 108.03, 77.36, 66.64, 26.03, 21.09, 21.05, 20.76, 20.64.

3. Results

3.1. Prediction of structural models

The closest homologues of NstcI were used as templates for homology modeling of NstcI and StcI enzymes. They were a heroin esterase from *Rhodococcus* sp. with 19% amino acid sequence similarity to NstcI [34] and a thermophilic esterase from *A. acidocaldarius* with 30% amino acid sequence similarity [35]. In spite of no significant sequence identity, this procedure was justified by the fact that all esterases belong to the same α/β hydrolase fold superfamily. Additionally, the positions of the amino acids from catalytic triad are in agreement with templates. This suggests that folding of both variants is correct.

Sequence analysis of StcI and NstcI performed at Lipase Engineering Database, LED [38] indicates the presence of the typical amino acid residues of the catalytic triad found in α/β hydrolases (Ser-152, Asp-255 and His-285) and the amino acid residues of the oxyanion hole (Gly-86 and Ala-153). The putative catalytic serine of both enzymes is predicted to reside in the amino acid sequence Gly-Ala-Ser-Ala-Gly (residues 150–154). The predicted structural models of the enzymes are clearly related to other esterases. NstcI has a single domain displaying the canonical α/β hydrolase fold, common in esterases with a Ser/Cys-Asp/Glu-His catalytic triad. The comparison of the putative structural models for both forms shows that the additional N-terminal peptide forms a helix–loop–helix motif that partially covers the active site of NstcI (Fig. 2). The N-terminal motif covering the active-site pocket is characteristic of several esterases, as the heroin esterase (PDB 1LZL), some thermophilic esterases from Archaea (PDB 1EVQ, 1QZ3, 2C7B, 1JJI) and other esterases as brefeldin-A esterase from *B. subtilis* (1JKM). The structural model of StcI, in contrast, has not this motif covering the active site, thus exposing a large hydrophobic surface composed by residues from loop 88 to 92 and helix 216 to 223. Furthermore, helix 216–223 found in NstcI is lost in StcI, presumably by the lack of contacts with the N-terminal residues. In addition, loops 188–204 and 156–171 are completely disordered as a result of the collapse of helix 216–233 in StcI.

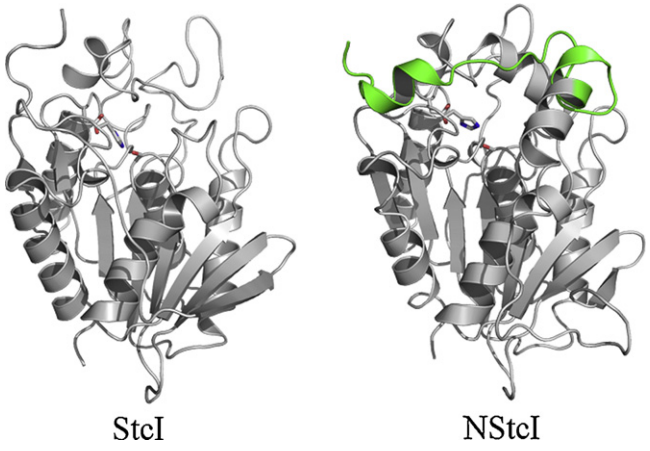

Fig. 2. Predicted structure models of StcI and NstcI. The additional 29 amino acids forming an α-helix are denoted in green. Amino acids from the active site (catalytic triad and oxyanion hole) are shown in blue and red. (For interpretation of the references to color in this figure legend, the reader is referred to the web version of the article.)

3.2. Expression in P. pastoris of stcI and nstcI genes

The RT-PCR products (945 bp for *nstcI* and 858 bp for *stcI*) were ligated into the pPICZα vector, generating pPICZα*nstcI* and pPICZα*stcI* plasmids. The identity of the cloned products was verified by sequencing. BLAST analysis revealed that the sequences of the RT-PCR products were identical to the corresponding *nstcI* and *stcI* gene sequences in Fig. 1. In the case of *nstcI*, we found the cDNA sequence without intron.

While high catalytically active protein was never obtained despite several attempts in *E. coli* (data not shown); an alternative host for heterologous expression was sought, *P. pastoris*. Plasmids were linearized with *Pme*I and *P. pastoris* X-33 was transformed. On the plates containing tributyrin, colonies harboring *nstcI* gene showed a bigger halo ring than clones harboring *stcI* gene. The presence in *P. pastoris* of the *stcI* or *nstcI* genes was corroborated by PCR using DNA from clones as template with AOX universal primers and sequencing. The results showed that the fragments corresponded to the *stcI* gene and *nstcI* gene and that they were in frame with the α-factor secretion signal sequence on the vector for extracellular expression.

For StcI expression, *P. pastoris* harboring the plasmid pPICZα*stcI* as integrating in its genomic DNA was cultivated in BMGY medium and then transferred to BMMY medium. At different times, samples were taken from the culture and assayed for cell growth and esterase activity (data not shown). After 48 h of induction, low esterase activity towards *p*-NFA (39 U/mg protein) was found and it was constant up to 72 h, and then decreased (data not shown). In the supernatant collected after 48 h of methanol induction, we have measured 13.9 U/mL with 0.355 mg protein/mL.

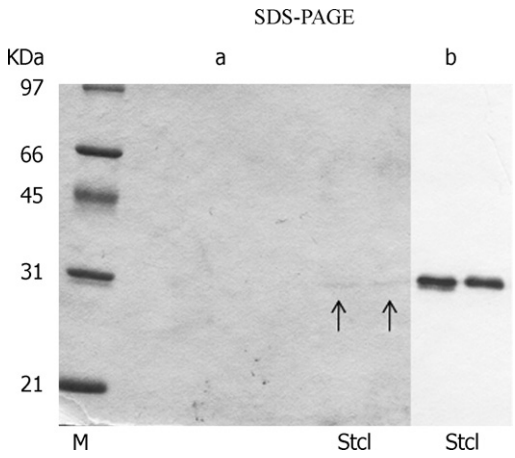

Fig. 3. Protein pattern and zymogram of extracellular extracts of recombinant clone expressing StcI protein. (a) Protein pattern on SDS-PAGE gel after coomassie staining. M, low molecular weight marker; StcI, crude extract of the recombinant clone expressing StcI protein. (b) Esterase activity after renaturation of StcI protein expressed by recombinant clone.

The ultrafiltered preparation was used for the purification of the recombinant enzyme. SDS-PAGE and zymogram analysis showed a single protein band having a molecular mass of 31 kDa which corresponds to the theoretically calculated value (31.19 kDa) with esterase activity (Fig. 3). The identity of the enzyme was corroborated also by western blot of native gel using specific antibodies (anti-StcI), which confirmed also the antibody specificity (Fig. 5). The enzyme has a pI of 5.3 which differs slightly from theoretically calculated value (4.91) (data not shown). Zymograms of native gel revealed two esterase activity bands, a stronger band with higher molecular mass and a weak band near to 31 kDa (Fig. 5).

For NstcI expression, *P. pastoris* harboring plasmid pPICZα*nstcI* was cultivated as before described. After 24 h of induction, high esterase activity towards *p*-NFA (360 U/mg protein) was detected and it was constant up to 96 h and then decreased (data not shown). In methanol induction phase, the maximum esterase activity measured in the supernatant was 189.7 U/mL with 0.527 mg protein/mL after 24 h of induction. SDS-PAGE and western blot analysis showed a single protein band having a molecular mass of 35 kDa which corresponds to the theoretical mass, 34.558 kDa (Fig. 4). The observed pI was approximately 4.5 lower to theoretical pI (4.84) (data not shown). Activity was detected only on native gels as a single band near to 35 kDa (Fig. 5).

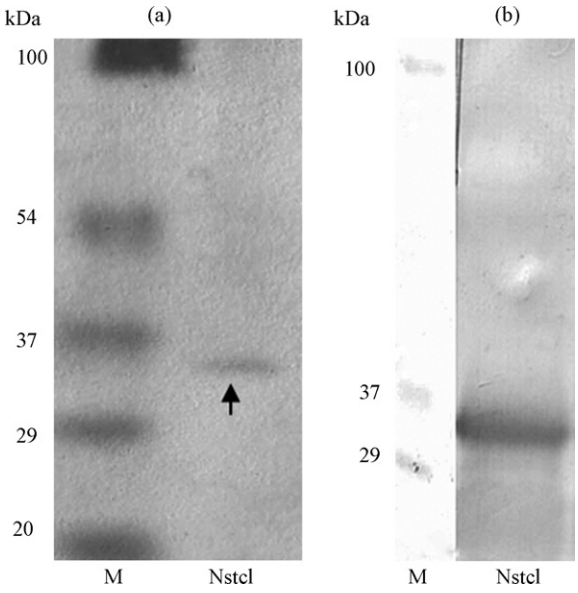

Fig. 4. Purified NstcI protein of extracellular extracts of recombinant clone. (a) Purified protein on SDS-PAGE gel after coomassie staining. M, low molecular weight marker; NstcI, purified recombinant NstcI protein. (b) Western blot analysis against recombinant NstcI protein on SDS-PAGE gel.

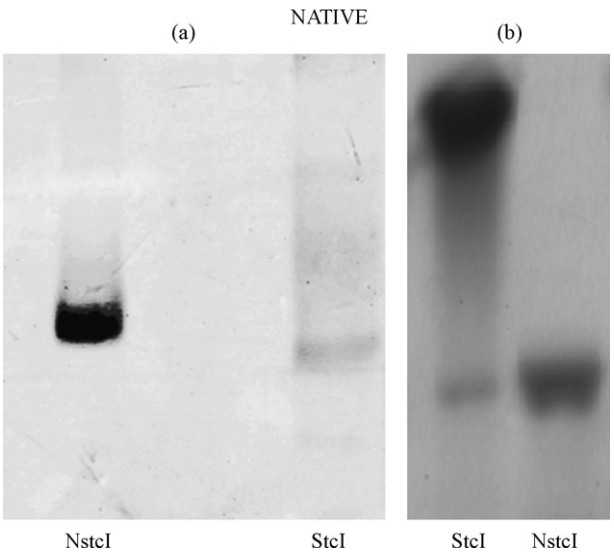

Fig. 5. Analysis of purified recombinant NstcI and StcI proteins on native gels. (a) Western blot analysis against purified recombinant NstcI and StcI proteins on native gels. (b) Esterase activity of purified recombinant proteins on native gels.

3.3. Effect of temperature and pH on esterase activity and stability

NstcI esterase was more active in temperature ranges of 30–50 °C, showing a maximum activity at 40 °C; while StcI esterase was more active in a range of 20–40 °C, showing a maximum activity at 30 °C. The thermostability of each enzyme was examined by measuring its residual activity after 30 min at pH 7.5. In these conditions, both enzymes retained up to 70% of their initial activity in the range of 20–40 °C. However, when the temperature was elevated to 50 °C, NstcI lost 50% of its initial activity, and StcI kept only 20% of its initial activity. Both enzymes were stable throughout 30 min incubation at the temperature where maximum activity was reached, 40 °C for NstcI and 30 °C for StcI (Fig. 6).

The effect of pH on NstcI activity at 37 °C was studied with *p*-NPA as the substrate. NstcI was active in the pH range of 7–9, while StcI was active between pH 6 and 8; the highest activity was found at pH 9 for NstcI and pH 8 for StcI. Using the pH-stat method for measuring activity, NstcI lost 80% of its activity at pH 10 (data not shown). The NstcI enzyme showed the highest activity at 37 °C, following 12-h incubation at pH 9, and was more stable in the pH range of 8–10. On the other hand, following 12-h incubation, StcI conserved its activity better at pH 9 than at other pH values, while its stability was better in the pH range from 7 to 9.

3.4. Different chain-length specificity for recombinant enzymes

The NstcI esterase was able to hydrolyze all *p*-nitrophenyl synthetic substrates evaluated showing higher activity than StcI in all cases. The highest activity (366 U/mg protein) was observed towards C2:0 chain-length *p*-nitrophenyl ester (*p*-NPA). In contrast, StcI esterase was able to hydrolyze all *p*-nitrophenyl synthetic sub-

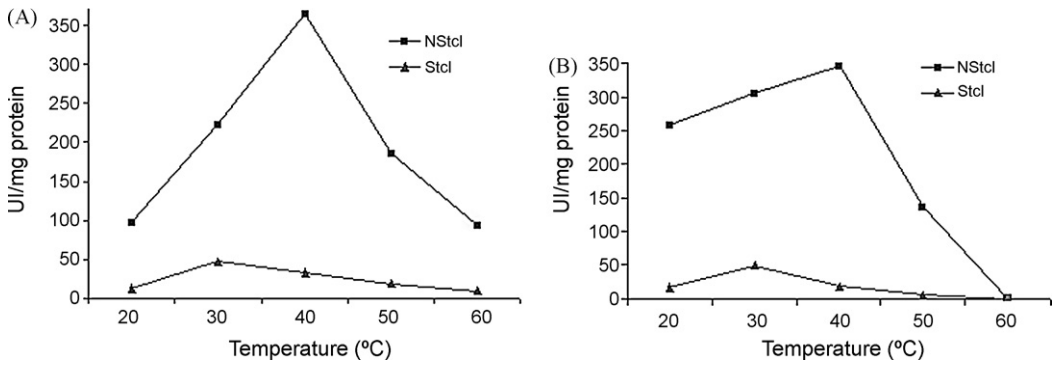

Fig. 6. Dependence of enzyme activity on temperature. NstcI (■) and StcI (▲). (a) Effect of temperature on esterase activity. (b) Effect of temperature on stability of the enzyme. Effects were determined by the spectrophotometric method using 50 mM phosphate buffer, pH 7.5. Results are the mean of three replicates.

Table 1
A. nidulans esterase-mediated deacetylation of different compounds in 48 h at 37 °C.

Group	Compound	Acetylated structure (Fig. 8)	Melting point (°C) of acetylated compound	*m/z* acetylated compound (g/mol)	*m/z* deacetylated compound (g/mol)	% conversion NstcI	% conversion StcI
Phenols I	Ferulic acid	**1a**	187	236	194	96	0
	α-Naphthol	**1b**	113	186	144	100	100
	TBHQ (tert-butyl hydroquinone)	**1c**	49	250	N/H	0	0
	Coumaric acid	**1d**	198	206	164	0	25
	Hydroquinone	**1e**	50	194	110	100	98
Aliphatic alcohols II	Phenyl ethanol	**1f**	105	164	122	0	30
	Kojic acid	**1g**	75	226	184	75	0
	β-Amyrin	**1h**	220	468	426	47	33
	Dihydrocholesterol	**1i**	87	428	N/H	0	0
Flavonoids III	Quercetin	**1j**	181	512	302	95	15
	Hesperetin	**1k**	108	485	302	100	20
	(+)Catechin	**1l**	102	500	290	100	63
	(−)Epicatechin	**1m**	135	444	290	60	23

N/H = no hydrolysis by StcI variants.

strates displaying the highest activity towards long chain-length *p*-nitrophenyl ester (*p*-NPS) (C18:0) (Fig. 7).

3.5. Deacetylation profile

Compounds having a structure similar to VHA (the original substrate of the enzyme) were tested as substrates for recombinant NstcI and StcI proteins. The structures of acetylated compounds are shown in Fig. 8. The results indicate that both recombinant enzymes, NstcI and StcI, have broad substrate specificity, but their substrate affinities are different. The results are summarized in Table 1, where the substrates are divided into three groups.

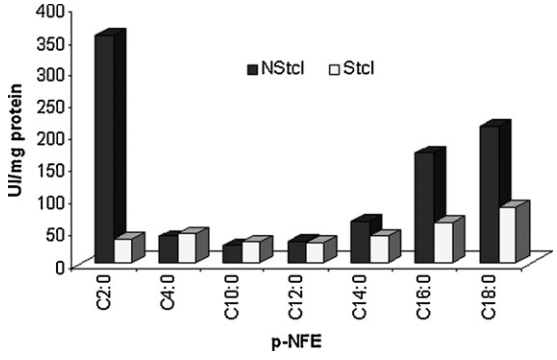

Fig. 7. Substrate preference. Substrate preference towards *p*-NP esters for NstcI (black) and StcI (light gray). Esterase activity on *p*-NPE was determined by the spectrophotometric method using 50 mM phosphate buffer, pH 7.5. Results are the mean of three replicates.

Group I (phenols), consists of compounds having higher structure similarity to VHA like *p*-NPA, α-naphthyl acetate and hydroquinone acetate. They were deacetylated with high efficiency (100%) by StcI and NstcI enzymes, as expected. This group includes also hydroxycinnamic acids. A difference in hydrolysis of these compounds was found: surprisingly, acetylated ferulic acid was hydrolyzed efficiently only by NstcI (96%), while StcI was shown to hydrolyze only acetylated coumaric acid (25%). In both cases, antioxidant activity was recovered after deacetylation of the compounds (data not shown). Hydrolysis of acetylated TBHQ was not detected under our assay conditions.

Among the substrates found in group II, both enzymes hydrolyzed β-amyrin with low yield. None of them hydrolyzed dihydrocholesterol. Phenyl ethyl acetate was hydrolyzed only by StcI with low yield (30%) and; interestingly, only NstcI hydrolyzed kojic acid (75%). This hydrolysis product was not fully deacetylated (data not shown). NMR analysis revealed that incomplete deacetylation was regioselective at position C5, which is the position that is regarded as important for recovery of antioxidant activity [39], a behavior that was observed with the stable free radical DPPH.

Flavonoids (group III) were efficiently hydrolyzed by NstcI (95–100%), with the lowest yield observed for epicatechin (60%).

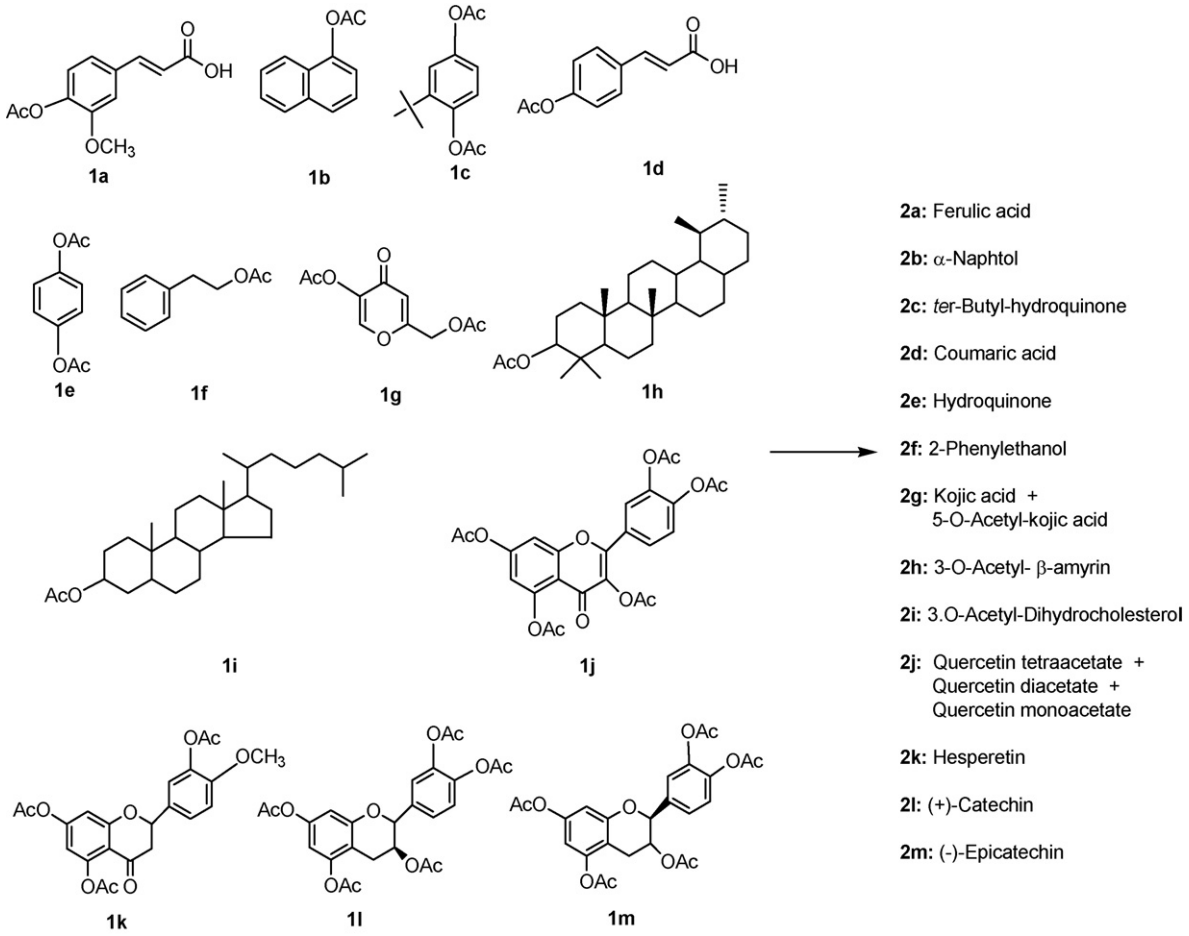

Fig. 8. Structures of compounds modified by NstcI and StcI. (1) Structure of acetylated compounds. (2) Structure of products obtained after deacetylation.

StcI deacetylated flavonoids less efficiently (15–20%), and the highest yield was found for catechin (63%). TLC experiments showed that the hydrolysis of quercetin produced different patterns of products for each enzyme. Antioxidant activity of flavonoids was recovered after deacetylation (data not shown).

4. Discussion

The structural models suggest that the active site of StcI is completely accessible to the solvent, while that of NstcI is partially covered by the additional residues at the N-terminus that builds up part of a lid or an elaborate active site cleft. These findings, together with the differences in activity towards several substrates, confirm that one of the roles of the N-terminus in NstcI is to modulate or discriminate substrate access to the active site. Thus, the lack of this motif will modify the chemo-, regio- and stereospecificity of the enzyme. In addition, this N-terminal motif may also play an essential role in stability. The hydrophobic surface exposed in StcI may induce protein aggregation as a result of hydrophobic interactions, as we have seen on native gels. Above and beyond, the overall lose of structure predicted for the StcI may dramatically reduce the core packing of the molecule, which keeps the enzyme folded for long time. Differences in expression levels for both clones and slight differences in their response to pH and temperature changes support this idea. Furthermore, yields for almost all acetylated products tested and activity on typical esterase substrates were higher for the NstcI form.

There were no reports about biochemical and catalytic properties StcI enzyme. It has been reported by Brown as a putative lipase/esterase [1]. We have found that the NstcI variant is an esterase, while the StcI as reported by Brown present lipase-like features. This finding is strongly correlated with the role of the N-terminus. Few investigations have been undertaken on the role of N-terminal region in enzyme substrate specificity. Sayari et al. found a shorter form of the 32 kDa lipase of *Rhizopus oryzae* after storing the culture medium at 0 °C for several months. This 29 kDa lipase lacked 28 amino acids from the N-terminal region and showed different regio- and stereoselectivity from the 32 kDa form [40]. Mandrich et al. reported an interesting structural study on the role of the N-terminus in the hormone sensitive lipase family highlighting the importance of the cap domain in several enzyme functions. They found different catalytic properties for a mutant of a thermophilic esterase belonging to the hormone sensitive lipase family, in which 35 amino acids from its N-terminal end were removed. This 35-amino acid region formed a cap domain that covered the active site in the wild type enzyme. They have found that after the removal of a cap domain it was clear that this deletion open the access to the active site and therefore should favor activity against long chain triglycerides which confers lipase-like features [41]. Interestingly, we have found also differences in the hydrolysis of *p*-NPE after removal of residues 1–29 of NstcI as NstcI displayed the highest activity towards short chain-length *p*-NFE (*p*-NPA) while StcI displayed the highest activity towards long chain-length *p*-NFE (*p*-NPS). Similar results were obtained with ethyl esters with acyl group chain-lengths from

C4:0 to C16:0. Our results are in accordance with the previously obtained by Mandrich with other esterase. The structural model for NstcI showed also this cap domain at the N-terminus covering the active site. Moreover, it has been reported that in the hydrolase family of enzymes, insertions are commonly observed in the canonical structure at the amino and carboxyl termini. Such insertions are believed to modulate the substrate specificity of the enzyme [34]. NstcI has one predominantly helical, 29-amino acid insertion at the amino terminus ant it modulate substrate specificity.

In the case of phenols, it was clear that the presence the tert-butyl group is a steric impediment for the hydrolysis, as the results were negative for both forms and in the absence of this, the hydrolysis was very efficient. Another important functional group is the hydroxyl group in the case of ferulic and coumaric acids. Its absence in coumaric hinders deacetylation by NstcI.

The yield percentages were generally higher for flavonoid compounds, and in all cases, the complete form (NstcI) displayed more activity. Interestingly, these compounds have at least three rings (bulky part), which have a structure similar to VHA, the substrate in the biosynthetic via. As TLC showed different products for this group, the pattern of deacetylation needs to be determined. In TLC, we could observe that this was different from *C. antarctica*.

In the case of aliphatic alcohols and phenols, the results were more heterogeneous for both enzymatic forms. As such, cholesterol and the TBHQ nucleus were not recognized by either. Amyrin is the bulkier form, and this was hydrolyzed by both enzymes in similar proportions. In order to clarify the differences in these behaviors, it is important to carry out crystallization of the enzyme and perform docking experiments.

The difference in chemoselectivity of these enzymes may be useful for biotechnological processes, and an interesting example is the selectivity difference found between substrates of group II (hydroxycinnamic acids). This result strongly suggests that protein engineering may be used to modify the N-terminal segment of NstcI to change the regio- or chemoselectivity of this or other enzymes. In case of flavonoid deacetylation, an industrially important biotransformation, where few enzymes capable of this function have been reported, it must be noted that the products obtained with the NstcI form are comparable to those reported for *C. antarctica* lipase [16]. Assay conditions may be manipulated in order to increase yields.

5. Conclusions

We found an additional 29-amino acid N-terminal region of the already reported *stcI* gene. Predicted structural models suggested that this N-terminus modifies substrate access to the active site, this was corroborated after experimental work; as we observed differences in the hydrolysis of *p*-NPE, in chemoselectivity for deacetylation of phenols, kojic acid and flavonoid esters and also in regioselectivity for the deacetylation of kojic acid and flavonoids. Moreover, this region is also important for the stability of the enzyme, as we have always obtained higher activity for NstcI protein and we observed slight differences in their response to pH and temperature.

Acknowledgments

CPM received a scholarship from DAAD, Germany which allowed collaboration with the ITB, University of Stuttgart. We appreciate the help of American Journal Experts (www.journalexperts.com) for their assistance with the English revision of this manuscript.

References

[1] D.W. Brown, J.H. Yu, H.S. Kelkar, M. Fernandes, T.C. Nesbitt, N.P. Keller, T.H. Adams, T.J. Leonard, Proc. Natl. Acad. Sci. U.S.A. 93 (1996) 1418–1422.
[2] J. Yu, P.K. Chang, D. Bhatnagar, T.E. Cleveland, Mycophatologia 156 (2002) 227–234.
[3] P.K. Chang, K. Yabe, J. Yu, Appl. Environ. Microbiol. 70 (2004) 3593–3599.
[4] B.A. Roe, D. Kupfer, H. Zhu, S. Gray, R. Clifton, J. Prade, J. Loros, J. Dunlap, M. Nelson. Available via: http://www.genome.ou.edu/asper_blast.html, 2001 (accessed 23.01.08).
[5] J.D. Bendtsen, H. Nielsen, G. von Heijne, S. Brunak, J. Mol. Biol. 340 (2004) 783–795.
[6] H. Morishita, M. Ohnishi (Eds.), Absorption, Metabolism and Biological Activities of Chlorogenic Acids and Related Compounds, Elselvier Science, Oxford, UK, 2001, pp. 919–953.
[7] F.A.M. Silva, F. Borges, C. Guimaraes, J.F.L.C. Lima, C. Matos, S. Reis, J. Agric. Food. Chem. 48 (2000) 2122–2126.
[8] M.A. Carbonneau, C.L. Le'ger, B. Descomps, F. Michel, L. Monnier, J. Am. Oil Chem. Soc. 75 (1998) 235–240.
[9] M. Serafini, G. Maiani, A. Ferro-Luzzi, J. Nutr. 128 (1998) 1003–1007.
[10] M.C. Figueroa-Espinoza, P. Villeneuve, J. Agric. Food Chem. 53 (2005) 2779–2787.
[11] K.E. Jaeger, B.W. Dijkstra, M.T. Reetz, Annu. Rev. Microbiol. 53 (1999) 315–351.
[12] U.T. Bornscheuer, FEMS Microbiol. 26 (2002) 73–81.
[13] R.D. Schmid, R. Verger, Angew. Chem. Ind. 37 (1998) 1608–1633.
[14] V. Gotor-Fernandez, R. Brieva, V. Gotor, J. Mol. Catal. B: Enzym. 40 (2006) 111–120.
[15] L. Chebil, C. Humeau, A. Falcimaigne, J.M. Engasser, M. Ghoul, Process Biochem. 41 (2006) 2237–2251.
[16] D. Lambusta, G. Nicolosi, A. Patti, C. Sanfilippo, J. Mol. Catal. B: Enzym. 22 (2003) 271–277.
[17] V.S. Parmar, H.N. Pati, A. Azim, R. Kumar, K.S. Bisht, A.K. Prasad, W. Errington, Bioorg. Med. Chem. 6 (1998) 109–118.
[18] V.S. Parmar, A. Kumar, H.N. Pati, R.K. Saxena, S. Davidson, R. Gupta, Biochim. Biophys. Acta 1387 (1998) 325–330.
[19] M. Natoli, G. Nicolosi, M. Piatelli, J. Org. Chem. 57 (1992) 5776–5778.
[20] J. Sambrook, E.F. Fritsch, T. Maniatis, Molecular Cloning: A Laboratory Manual, third ed., Cold Spring Harbor Laboratory Press, New York, 2001.
[21] K. Isobe, T. Akiba, S. Yamaguchi, Agric. Biol. Chem. 52 (1988) 41–47.
[22] U.K. Laemmli, Nature 227 (1970) 680–685.
[23] J.E. Galagan, S.E. Calvo, C. Cuomo, L.J. Ma, J.R. Wortman, S. Batzoglou, S.I. Lee, M. Baştürkmen, C.C. Spevak, J. Clutterbuck, V. Kapitonov, Nature 438 (2005) 1105–1115.
[24] S.E. Douglas, Methods Mol. Biol. 25 (1994) 181–194.
[25] M.A. Larkin, G. Blackshields, N.P. Brown, R. Chenna, Bioinformatics 23 (2007) 2947–2948.
[26] T. Hall, BioEdit Biological Sequence Alignment Editor for Win95/98/NT/2K/XP. Available via: http://www.mbio.ncsu.edu/BioEdit/bioedit.html, 2007 (accessed 29.01.07).
[27] D. DeCaprio, J.P. Vinson, M.D. Pearson, P. Montgomery, M. Doherty, J.E. Galagan, Genome Res. 17 (2007) 1389–1398.
[28] C.B. Burge, S. Karlin, Curr. Opin. Struct. Biol. 8 (1998) 346–354.
[29] E. Gasteiger, A. Gattiker, C. Hoogland, I. Ivanyi, R.D. Appel, A. Bairoch, Nucleic Acids Res. 31 (2003) 3784–3788.
[30] C. Lambert, N. Leonard, X. De Bolle, E. Depiereux, Bioinformatics 18 (2002) 1250–1256.
[31] G.J. Vriend, Mol. Graph. 8 (1990) 52–56.
[32] L.J. McGuffin, D.T. Jones, Bioinformatics 19 (2003) 874–881.
[33] D.T. Jones, J. Mol. Biol. 292 (1999) 195–202.
[34] X. Zhu, N.A. Larsen, A. Basran, N.C. Bruce, I.A. Wilson, J. Biol. Chem. 278 (2003) 2008–2014.
[35] G. De Simone, L. Mandrich, V. Menchise, V. Giordano, F. Febbraio, M. Rossi, C. Pedone, G. Manco, J. Biol. Chem. 279 (2004) 6815–6823.
[36] N. Peled, M.C. Krenz, Anal. Biochem. 112 (1981) 219–222.
[37] E. Forgacs, T. Cserhati, J. Liq. Chromatogr. Rel. Technol. 25 (2002) 1521–1541.
[38] M. Fischer, J. Pleiss, Nucleic Acids Res. 31 (2003) 319–321.
[39] H.S. Rho, H.S. Baek, J.W. You, Bull. Korean Chem. Soc. 28 (2007) 471–473.
[40] A. Sayari, F. Frikha, N. Miled, H. Mtibaa, Y. Ben Ali, R. Verger, Y. Gargouri, FEBS Lett. 579 (2005) 976–982.
[41] L. Mandrich, L. Merone, M. Pezzullo, L. Cipolla, F. Nicotra, M. Rossi, G. Manco, J. Mol. Biol. 345 (2005) 501–512.

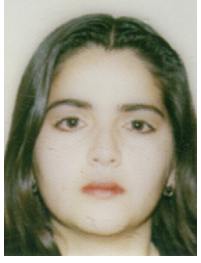

Carolina Peña-Montes She studied Food Chemistry at the National Autonomous University of Mexico (UNAM), later in Faculty of Chemistry (UNAM), where she obtained her MSc Biochemistry and Biotechnology degree. She worked as patent examiner at the Institute of Industrial Property. During her PhD studies, she obtained a grant from DAAD for working in Prof. Schmid's laboratory in the Institute of Technical Biochemistry at the University of Stuttgart, where she worked for 2 years. She is in process to obtain her PhD in Biochemistry Sciences degree. Actually, she works at UNAM as academic technician at the food and biotechnology department.

Dr. Stefan Lange Dr. Stefan Lange is Senior Team leader at Roche Molecular Diagnostics in Rotkreuz, Switzerland where he focuses on test development, e.g. the recently launched CE marked MRSA Advanced test. Before joining Roche Diagnostics in 2007, Stefan worked for more than a decade at the Institute of Technical Biochemistry at the University of Stuttgart, Germany where he received a Diploma (1997) and a PhD (2002) in "Technical Biology". Research interests and topics of numerous publications in international journals and conferences include recombinant expression and directed evolution of enzymes and antibodies, exploration of metagenomes for industrial enzymes, biocatalysis, and systems biology.

Denise Castro-Ochoa Denise Castro studied Biochemical Engineering at Los Mochis Institute of Technology, Sinaloa, México, later she obtained her MSc Biochemical Engineering Sciences degree at Veracruz Institute of Technology, Veracruz, México. Thesis title: Screening, purification and characterization of the thermoalkalophilic lipase produced by *Bacillus thermoleovorans* CCR11. Actually she is studying at the National Autonomous University of México (UNAM) to obtain her PhD in Biochemistry Sciences degree, working under the supervision of Dr. Amelia Farrés.

Katia Ruiz-Noria Katia Ruiz-Noria studied Food Chemistry at the National Autonomous University of Mexico (UNAM). Her thesis work was done in Amelia Farres's laboratory focused in enzymatic biocatalysis. She has experience in HPLC and Gas Chromatography. Actually she is working for the food industry.

Dr. Felipe Cruz-García Felipe Cruz studied Biology at UNAM, later he obtained his Dr. Chemistry Sciences (Biochemistry) degree in 1997 at UNAM. He worked in the Department of Molecular Genetics of the University of Missouri-Columbia (USA) from 1997 to 1999 during his postdoctoral studies in Bruce McClure's laboratory. Actually he works at the Biochemistry Department of Chemistry Faculty, UNAM. 12 graduate students have obtained their degree under his supervision. His research work is focused in plant biochemistry.

Dr. Rolf Schmid Rolf Schmid studied Chemistry at the University of München, later in Freiburg, where he obtained his Dr. rer. nat. degree in 1970 for thesis work done in Hans Griesebach's laboratory. After postdoctoral studies in France and the USA, he joined the research laboratories of Henkel KGaA in Düsseldorf where he became Director of the Biotechnology Laboratories. In 1987, he moved to the 'Gesellschaft für Biotechnologische Forschung' (GBF) in Braunschweig where he headed the Division of Enzyme Technology and Natural Products Research. In 1993, he built up the Institute for Technical Biochemistry at the University of Stuttgart.

Dr. Arturo Navarro-Ocaña Arturo Navarro Ocaña, born in Mexico City, received his PhD in Biotechnology from Mexico National University (UNAM), in his PhD working under the supervision of Eduardo Bárzana García in the area of biocatalysis/biotransformations. In 1998 after stay in Iowa University, Laboratory of Horacio Olivo in USA, he joined the chemistry faculty in the food and biotechnology department at the UNAM. His research is currently studying the fundamental and applied aspects of the food chemistry: food colorant an antioxidant, nutraceutical and functional food. Biocatalysis and biotransformations in organic synthesis: bioreduction of nitro and carbonyl groups and sterification with lipases the hydroxycinnamic acids and other natural molecules.

Dr. Amelia Farrés Amelia Farres is a Biologist from UNAM, Mexico, and a graduate in Biotechnology at the same University. Her research interests include several aspects in Food Biotechnology. Most of her publications are related to enzyme production and regulation. She works at the Chemistry Faculty from UNAM, where she headed the Department of Food and Biotechnology. 21 graduate students have obtained their degree under her supervision.